ELSEVIER

International Journal of Adhesion & Adhesives 24 (2004) 335–346

International Journal of Adhesion & Adhesives

www.elsevier.com/locate/ijadhadh

The effect of molecular weight and temperature on tack properties of model polyisobutylenes

Adrienne E. O'Connor[a,1], Norbert Willenbacher[b,*]

[a] Department of Chemical Engineering and Material Science, University of Minnesota, Minneapolis, MN 55455, USA
[b] BASF Aktiengesellschaft, Polymer Physics, G 201, 67056 Ludwigshafen, Germany

Accepted 14 November 2003

Abstract

The effect of molecular weight and temperature on the tack of non-crosslinked soft polymers was investigated using blends of low and high molecular weight polyisobutylene as model systems. Molecular weight between entanglements M_e was varied systematically by changing the mixing ratio. Video-optical imaging confirms that these model systems exhibit the characteristic debonding features of pressure-sensitive adhesives, including cavitation as well as formation and deformation of fibrils. The initial peak in the stress–strain diagram is a function of both the cohesive strength and ability to wet the probe. It contributes significantly to the work of adhesion at low molecular weight, low temperature and high contact force. Beyond a critical molecular weight, debonding is dominated by fibril deformation. In this regime, the work of adhesion is essentially independent of temperature, molecular weight and the details of the fibrillation pattern (more but thinner fibrils are observed as molecular weight increases). The minimum molecular weight needed for significant fibrillation is around 850 kg/mol ($\approx 3\,M_e$) both at -10°C and 25°C.

Keywords: A. Pressure-sensitive; B. Rheology; C. Tack; D. Viscoelasticity

1. Introduction

Pressure-sensitive tack is not precisely defined, but it can be described as the property of an adhesive that enables it to form a bond of measurable strength upon brief contact with another surface under light pressure [1]. It is an "instantaneous" adhesion, and it is the property of pressure-sensitive adhesives (PSAs) that sets these materials apart from other types of adhesives. Tack, which is inversely proportional to the elasticity modulus, should be high enough that the adhesive surface achieves bonding from merely contacting and pressing to a substrate. The tack also provides resistance of an adhesive film to detachment from a substrate [2–4]. A simple method of measuring properties of soft adhesives is a tack test with a flat cylindrical probe [5].

The strength of an adhesive bond is determined by the thermodynamic contributions to the interfacial energy (van der Waals interactions, electrostatic forces, and hydrogen bonding) and the rheological contributions due to the viscoelastic dissipation during deformation of the polymer chains in the adhesive layer itself [6]. The total work of adhesion, W, is described by

$$W = W_A(1 + \Phi), \tag{1}$$

where W_A is the intrinsic work of adhesion, and Φ describes the effect of the rheological properties of the material [7,8]. The contribution of Φ can be very large, depending on the test conditions chosen. In a tack test, the work of adhesion is dominated by this viscoelastic contribution.

Most PSAs are blends of numerous components, including elastomers, tackifiers, plasticizers, and fillers [9]. Because of the complexity of these materials, it can be difficult to quantify the effect of a single variable, such as molecular weight, on the adhesive properties. Tobing and Klein have extensively studied the relationship between molecular architecture, mainly network topology and crosslinking, and adhesive properties

*Corresponding author. Fax: +49-621-6043832.
E-mail address: norbert.willenbacher@basf-ag.de (N. Willenbacher).
[1] Current address: Degussa Construction Chemicals, Shakopee, MN 55379, USA.

0143-7496/$ - see front matter © 2004 Elsevier Ltd. All rights reserved.
doi:10.1016/j.ijadhadh.2003.11.005

using carefully characterized acrylic polymers from solution and emulsion polymerization [10,11].

In this paper we focus on the effect of molecular weight on the adhesive behavior of a PSA. To that end we have studied model systems of polyisobutylene (PIB) homopolymers without any additives. PIB possesses great flexibility and is completely amorphous with a glass-transition temperature of $-65^{\circ}C$. The entanglement molecular weight (M_e) of PIB is 8.7 kg/mol. High-molecular-weight grades ($M_v > M_e$) are strong and elastic; they do not show fibrillation [12] and can serve as the elastomeric base of a model PSA [13]. However, low-molecular-weight PIB ($M_v < M_e$) is very soft and liquid-like, making it a suitable tackifier.

We have investigated mixtures of low and high molecular weight PIB as model systems showing cavitation and fibrillation typical of PSAs. This choice of model system enables studying the effect of molecular weight on tack independent from the contributions due to crosslinking, gel content or network topology. Molecular weight between entanglements is changed systematically by variation of the mixing ratio. Our model systems are not true PSAs, but the results of this should generally apply to systems based on PIB, acrylic polymers, block copolymers, or any variety of PSA.

2. Experimental

Blends of low- and high-molecular-weight commercial-grade Oppanol polyisobutylene (BASF AG, Ludwigshafen, Germany) were prepared at concentrations of 40%, 80% and 90% by weight of a low-molecular-weight component (1.5 kg/mol). Polymer films for tack testing were cast from solution of the PIB mixtures in light mineral oil onto glass slides using a doctor blade to create a uniform layer of adhesive. In all cases final film thickness was approximately 70 μm. Rheological measurements were made on an ARES strain-controlled rheometer (Rheometrics Inc.) using 8-mm plates and a nominal 1-mm gap. Samples trade names, the designations used in this paper and viscosity-average molecular weights (M_v) are given in Table 1. All of the polymers except the sample of the lowest molecular weight (Sample B1) are above M_e. Thus, adding B1 increases the molecular weight between entanglements in these adhesives.

All tack measurements were performed using a Texture Analyzer TAXT2i (Stable Micro Systems, UK). Testing occurred at temperatures of $-10^{\circ}C$ and $25^{\circ}C$, controlled using a peltier plate. The sample was placed in a chamber filled with nitrogen to prevent water condensation on the adhesive. A flat probe was chosen since it establishes a more uniform stress distribution and thus promotes the occurrence of fibrillation [14]. The adhesive film was positioned below a cylindrical stainless-steel probe with a diameter of 2 mm. The probe contacted the adhesive with a specified force, after which it was held at a constant position for a controlled amount of time. The probe was then withdrawn at a constant rate, and the resulting force curve was recorded.

Table 1
Molecular weight of PIB polymers. Trade name of BASF is Oppanol® BX

Trade name	Label in this paper	M_v (kg/mol)
B3	B1	1.5
B15	B88	88
B50	B395	395
B80	B850	850
B100	B1170	1170
B150	B2740	2740
B200	B3630	3630
B246	B6650	6650

In all tests, the probe approached the sample at a rate of 0.1 mm/s and withdrew from the sample at 1.0 mm/s. Contact time was 1.0 s, and contact force was varied from 0.5 to 5.0 N. Variations in contact force, temperature, and sample composition were investigated.

Video images were obtained with a CCD camera using Zosel's tack apparatus, described elsewhere [8,15]. The camera was mounted below a PIB-coated glass slide. The slide and adhesive layer are transparent, allowing monitoring of the contact area and deformation during a probe tack test in real time.

A shear holding power test was used, in which a 0.25-in^2 area of adhesive tape was applied to a stainless-steel panel. The bond was allowed to strengthen for 10 min at $25^{\circ}C$ before using a weight-distributing clip to hang a 500-g mass from the tape. This test was conducted according to the FINAT Test Method for Resistance to Shear from a Standard Surface (FTM 8, 2001), substituting the 500-g weight for the 1-kg weight specified due to the short holding times of these adhesives.

3. Results

3.1. Rheological characterization

Fig. 1 shows the rheological behavior of several PIB samples as a function of temperature. The transition from unentangled (B1) to slightly entangled (B88) and finally to highly entangled polymer melts (B395 and B1170) clearly shows up in the temperature dependence of G' and G''.

Fig. 2(a) illustrates the decrease in entanglement molecular weight for varying fractions of B1 blended with B3360. The mechanical behavior in the temperature

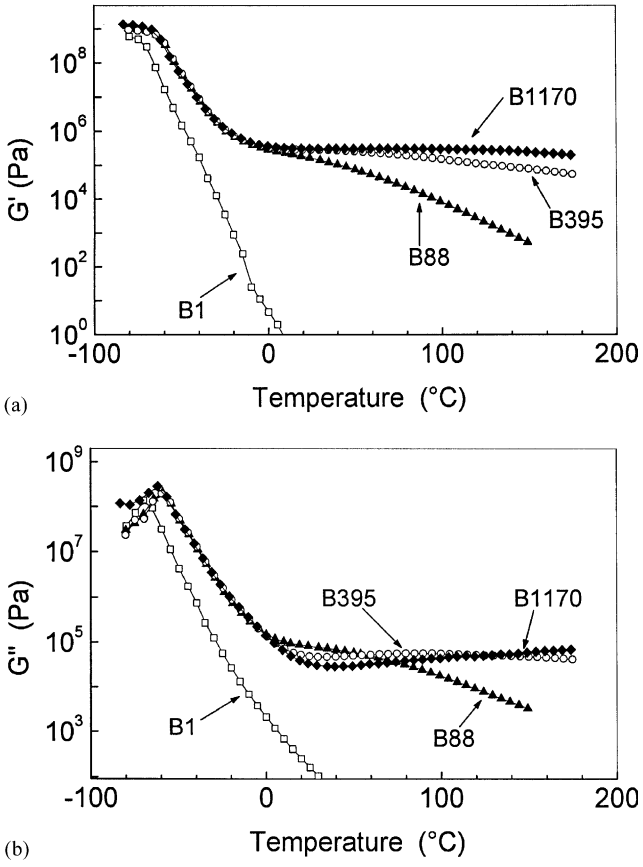

Fig. 1. Shear modulus of PIBs as a function of temperature (oscillation frequency $f = 1$ Hz), (a) storage modulus G', (b) loss modulus G''. Molecular weights indicated are in kg/mol.

range above T_g is governed by molecular entanglements [8]. The entanglement molecular weight (M_e) was calculated from the plateau modulus (G_N^0), according to the following equation:

$$M_e = \rho RT/G_N^0. \quad (2)$$

The M_e values are given in Fig. 2(a). Only the blends of B1/B3630 are shown, but the M_e values will be the same for all samples of the same blend ratio. As additional low-molecular-weight polymer is added, the plateau modulus drops accordingly. The 90/10-blend modulus is very low, consistent with the very sticky, low cohesiveness of the material. Dahlquist [16] correlated tack with the compliance of an adhesive, concluding that good tack is achieved when the compliance is at least $10^{-6}\,\mathrm{Pa}^{-1}$ after 1 s of compression. This is equivalent to requiring $G' < 3.3 \times 10^5$ Pa at low frequency. All of the blends are clearly below the Dahlquist criterion for tack.

When any of the various high-molecular-weight polymers are blended with the low-molecular-weight PIB, the number of entanglements decreases per unit volume. Fig. 2(b) shows that above T_g, all of the entangled 80/20 PIB blends display the same plateau modulus values, but the plateau modulus extends

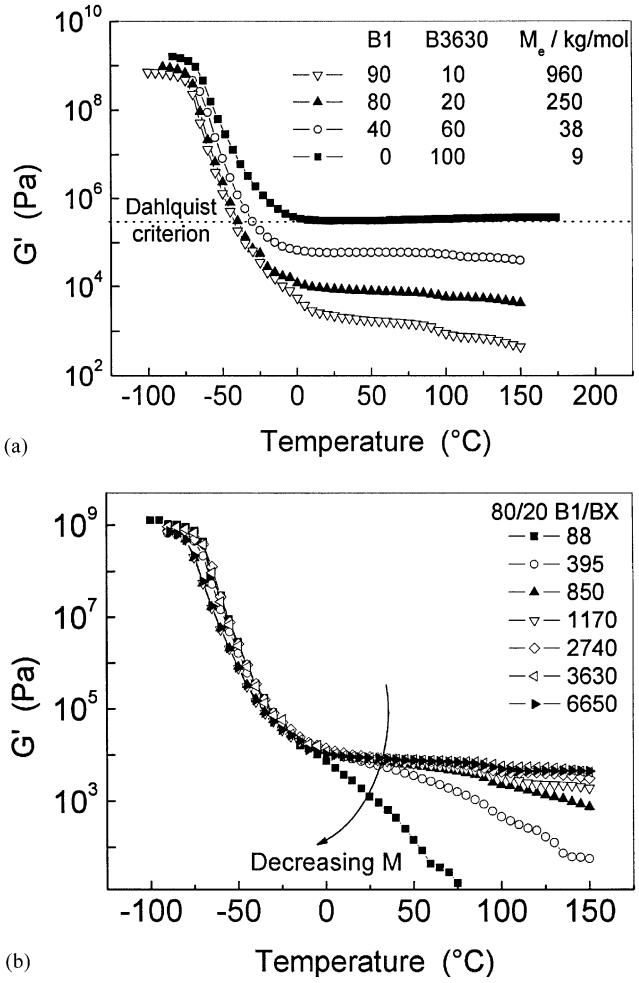

Fig. 2. Storage moduli of PIB blends ($f = 1$ Hz): (a) B3630 with varying amounts of B1 and (b) 80% B1 with varying molecular weight of the second component.

further for higher molecular weights. The B88 sample does not show any effective plateau since it is essentially not entangled due to the addition of 80% B1.

3.2. Video-optical characterization of debonding

The deformation of an adhesive during probe withdrawal occurs in the following order: appearance of cavities on the probe surface; lateral growth of the cavities; and extensional growth of the cavities until fracture or debonding [17]. Each of these three stages is illustrated by the video frames in Fig. 3, which show the evolution of the cavities and fibrils during a tack test on an 80/20 blend of B1/B6650. The corresponding stress response is plotted as a function of time, as the probe is withdrawn at a rate of 1.0 mm/s.

When the probe is withdrawn, cavities appear randomly on the surface, shown by the first image in Fig. 3, reducing the load-bearing area and thus the stress. Gradually, as deformation continues, air is drawn in from the outside as the outermost fibrils become

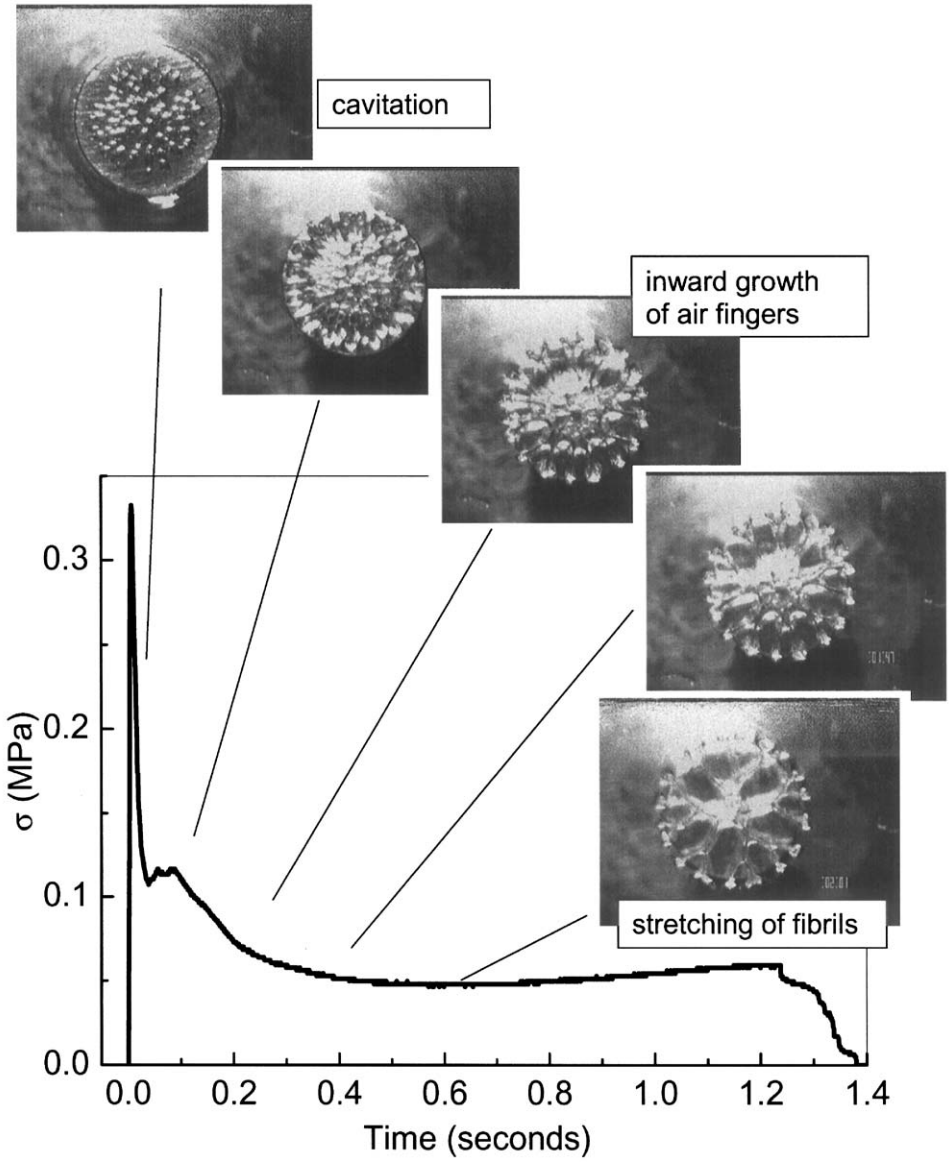

Fig. 3. Cavitation and fibrillation related to characteristic debonding curve of an 80/20 blend of B1/B6650 at 25°C, $F_c = 5$ N, dwell-time $t_d = 1$ s, debonding rate $v_d = 1$ mm/s.

thinner and break, and "fingers" of air penetrate to the center of the probe. As illustrated, this can create a second small peak after the first initial tack peak. This minor peak has also been observed by Lakrout and coworkers [18], when the walls between cells yield to outside pressure and allow air penetration. The progression of these fingers to the center of the probe leads to the formation of separated fibrils and each cavity achieves a steady-state cross-sectional area. Fibril elongation is facilitated by the decreasing wall thickness and flow from the base of the fibrils during the long plateau observed. The energy required to continue extending the fibrils will eventually exceed the adhesion between the PSA and the probe, and failure will occur through cohesive fracture or by separation of the adhesive from the probe surface.

3.3. Effect of contact force

A typical stress–strain diagram resulting from a tack experiment is shown in Fig. 3. Four parameters are determined to describe these curves quantitatively: the initial stress peak σ_p, the stress level σ_s at the shoulder which is typical for PSAs, the deformation at break ε_B and finally, the work of adhesion W_{adh}, which is determined from the area under the curve. The effect of contact force F_c on these parameters is shown in Fig. 4 for the 80/20 mixture of B1 and B1170. Similar results have been obtained for other blends. Fig. 5 shows images of the polymer films 20 ms after the start of debonding. Obviously, F_c has a strong impact not only on σ_p, which varies by a factor of 4 in the investigated force range, but also on the number of cavities formed,

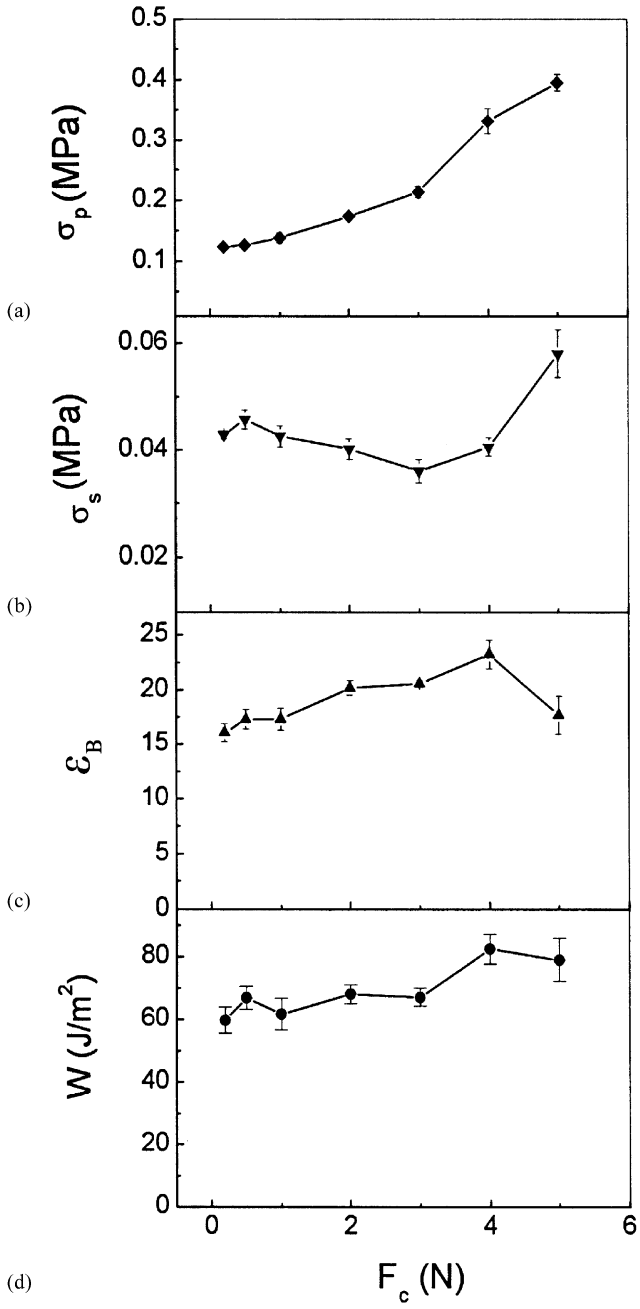

Fig. 4. Characteristic parameters σ_p, σ_s, ε_B, and W_{adh} of stress strain curve for the 80/20 blend of B1 and B1170 at $T=25°C$ as a function of contact force (dwell-time $t_d=1$ s, debonding rate $v_d=1$ mm/s).

which decreases substantially with increasing contact force. On the other hand, σ_s and ε_B, which are related to fibril deformation, do not change systematically and vary only by about 30%.

3.4. Effect of molecular weight between entanglements

Decreasing the ratio of the low-molecular-weight PIB (B1) to the high-molecular-weight component (BX) lowers the molecular weight between entanglements and therefore creates an adhesive with greater cohesive strength. In Fig. 6, stress–strain diagrams for various mixtures of low and high molecular weight PIB are shown for the blend ratios 80/20 and 40/60. For the 40/60 blend ratio, a distinct stress shoulder corresponding to fibrillation is only found for the lowest molecular weight (B88). Furthermore, films with a blend ratio of 90/10 have also been investigated, but these polymers were too soft and only few weak fibrils formed providing little resistance to flow. This resulted not in real shoulders but long "tails" in the stress–strain diagram, which did not contribute much to the work of adhesion (diagrams not shown). Thus, the following investigations regarding the effect of molecular weight on tack are focused on the 80/20 blend ratio.

3.5. Effect of molecular weight

The tack properties of a series of blends composed of 80% B1 and 20% of a higher-molecular-weight PIB were tested at 25°C at three different contact forces. Samples are referred to by the identity of the high-molecular-weight component. Representative curves for these tests are shown in Fig. 6(a) for a contact force of 2.0 N. Trends in the average tack properties are plotted as a function of the second-component molecular weight in Figs. 7a–d at three contact force values.

The peak stress σ_p is related to the wetting and the contact formation between adhesive and substrate. As already shown in Fig. 4, σ_p increases with increasing contact force. This effect is especially strong for the sample B88 but it diminishes as molecular weight increases.

The height of the shoulder σ_s and the elongation at break ε_B are parameters related to the formation of fibrils and reflect the cohesive strength of the PSA, but they also depend on the interfacial adhesion. Both parameters are essentially independent of contact force. For the lowest molecular weight (B88) almost no fibrils form (also illustrated by the stress–strain curve for B88 in Fig. 6) and consequently σ_s and ε_B are close to zero. For the blend including B395, σ_s is still small but ε_B reaches extraordinarily high values. This is because only a few weak fibrils with little resistance to flow are formed similar to the observations described in Section 3.4 for the 90/10 blends mentioned. Only the blends with molecular weight of 850 kg/mol or higher show the strong fibrillation typical for PSAs. In this range, ε_B slightly decreases with increasing molecular weight while σ_s strongly increases for M_v around 1000 kg/mol and tends to level off beyond 3000 kg/mol. The different debonding and fibrillation characteristics are also illustrated by the video images obtained during tack tests of samples composed of B88 and B1170, shown in Fig. 8. These images provide a clear contrast between the debonding behavior at high and low molecular

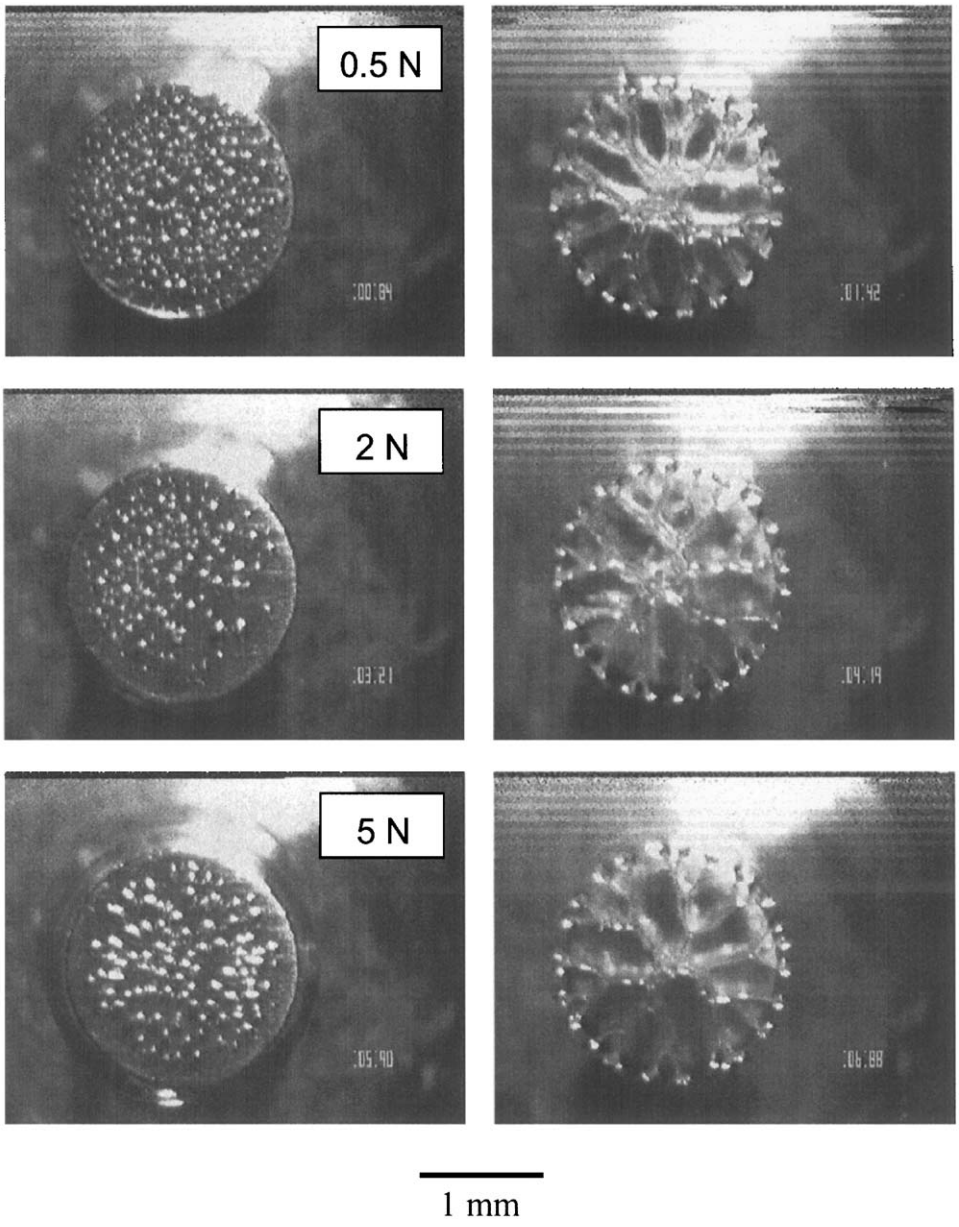

Fig. 5. Bottom view of the debonding pattern for the 80/20 blend of B1 and B1170 at $T = 25^{\circ}C$ for three different contact forces (dwell-time $t_d = 1$ s, debonding rate $v_d = 1$ mm/s): (top) 0.5 N, (middle) 2 N, (bottom) 5 N. left column: 20 ms after start of debonding, right column: immediately before failure.

weight. The sample with B88 does not show significant fibrillation; the cavities grow and coalesce with neighboring cells quickly. Around 200 ms after the appearance of cavities, the adhesive detaches from the probe and the film begins to return to its original state only 20 ms later. In the B1170 film, its higher viscosity impedes the growth of the air pockets within the plane parallel to the surface of the probe. Instead, the fibrils elongate and the cavities grow in length. This fibrillation makes a significant contribution to the work of adhesion during the tack test. The final image shows the pattern left in the film after the adhesive separates from the probe. Long polymer relaxation times lead to similar patterns in all of the higher-molecular-weight samples.

The work of adhesion W_{adh} is a function of the initial adhesion to the test probe as well as the ability of the PSA to dissipate energy during fibrillation and debonding. It is calculated from the area under the stress–strain curve. For high contact forces and low molecular weights, W_{adh} is dominated by the strong initial peak, which is a consequence of the good, pressure-induced wetting of these low viscosity fluids. But at molecular weights of 850 kg/mol and higher, W_{adh} is controlled by the deformation of the fibrils and the effect of contact

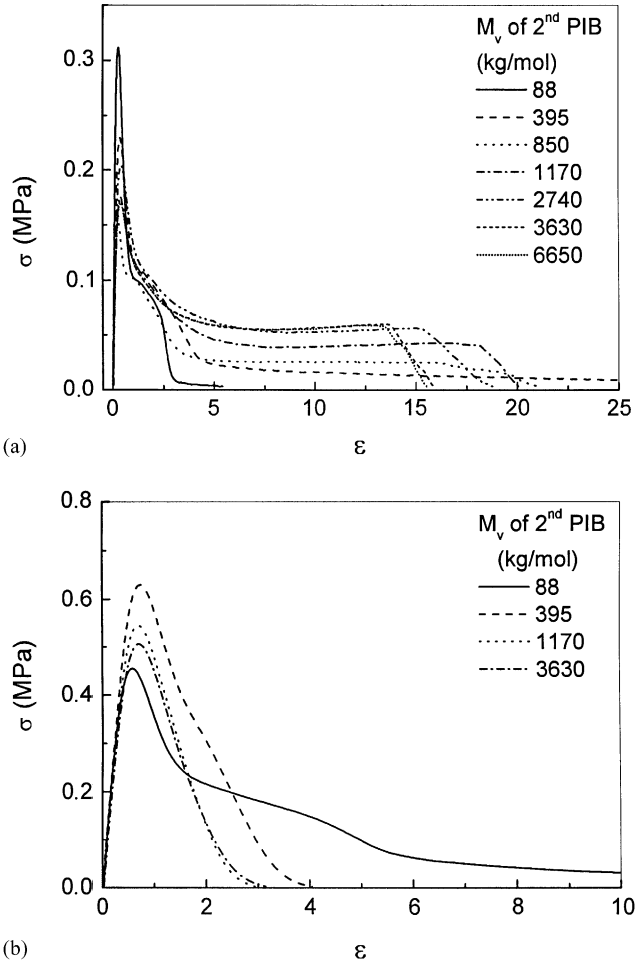

Fig. 6. Representative stress strain curves for B1/BX blends. (a) mixing ratio 80/20 (M_e = 255 kg/mol), (b) mixing ratio 40/60 (M_e = 38 kg/mol). Test conditions: T = 25°C, F_c = 2 N, dwell-time t_d = 1 s, debonding rate v_d = 1 mm/s.

force is small. In this range, which is most relevant for PSAs, W_{adh} is essentially independent of molecular weight.

3.6. Effect of temperature

The behavior of these model PIB systems was recorded at −10°C and compared to measurements at 25°C to determine the influence of temperature on the properties of adhesives with varying molecular weight. A contact force of 2.0 N was used for measurements discussed in this section.

Representative stress–strain curves for the series of 80/20 B1/BX blends at −10°C are shown in Fig. 9. It is clear from comparisons of these curves with the measurements at 25°C (Fig. 6(a)) that the cohesive strength of the films increases at lower temperatures. At −10°C, the fibrillation shoulders drop off more sharply preceding detachment of the adhesive from the probe, and final strain values are lower than at 25°C. Average

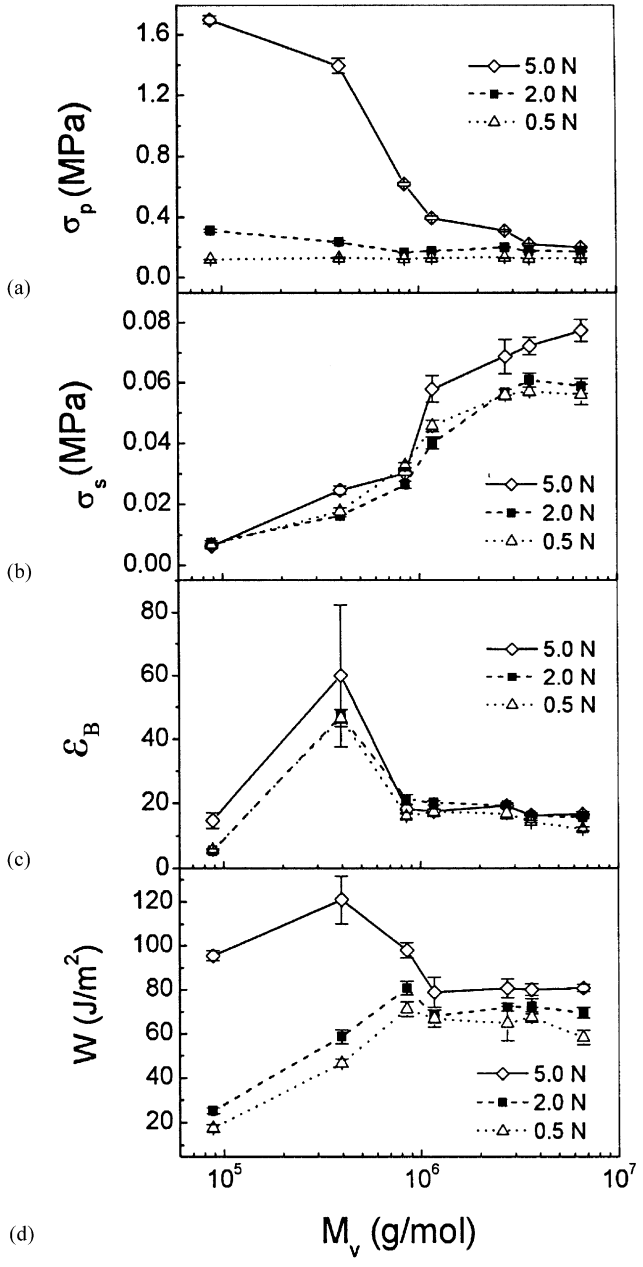

Fig. 7. Characteristic parameters σ_p, σ_s, ε_B, and W_{adh} of stress strain curve for the 80/20 blends Bl/BX as a function of M_v for different contact forces. Test conditions: T = 25°C, dwell-time t_d = 1 s, debonding rate v_d = 1 mm/s.

values for the characteristic parameters of the stress–strain curves at 25°C and −10°C are compared in Figs. 10(a)–(d).

While at 25°C σ_p decreases from 0.3 to 0.15 MPa when molecular weight increases, the values at −10°C scatter around 0.3 MPa and no clear trend with M_v is seen. At −10°C fibrillation is observed and a significant shoulder in the stress–strain diagrams is detected for all blends even at the lowest molecular weight. The stress level at the shoulder is consistently higher at −10°C

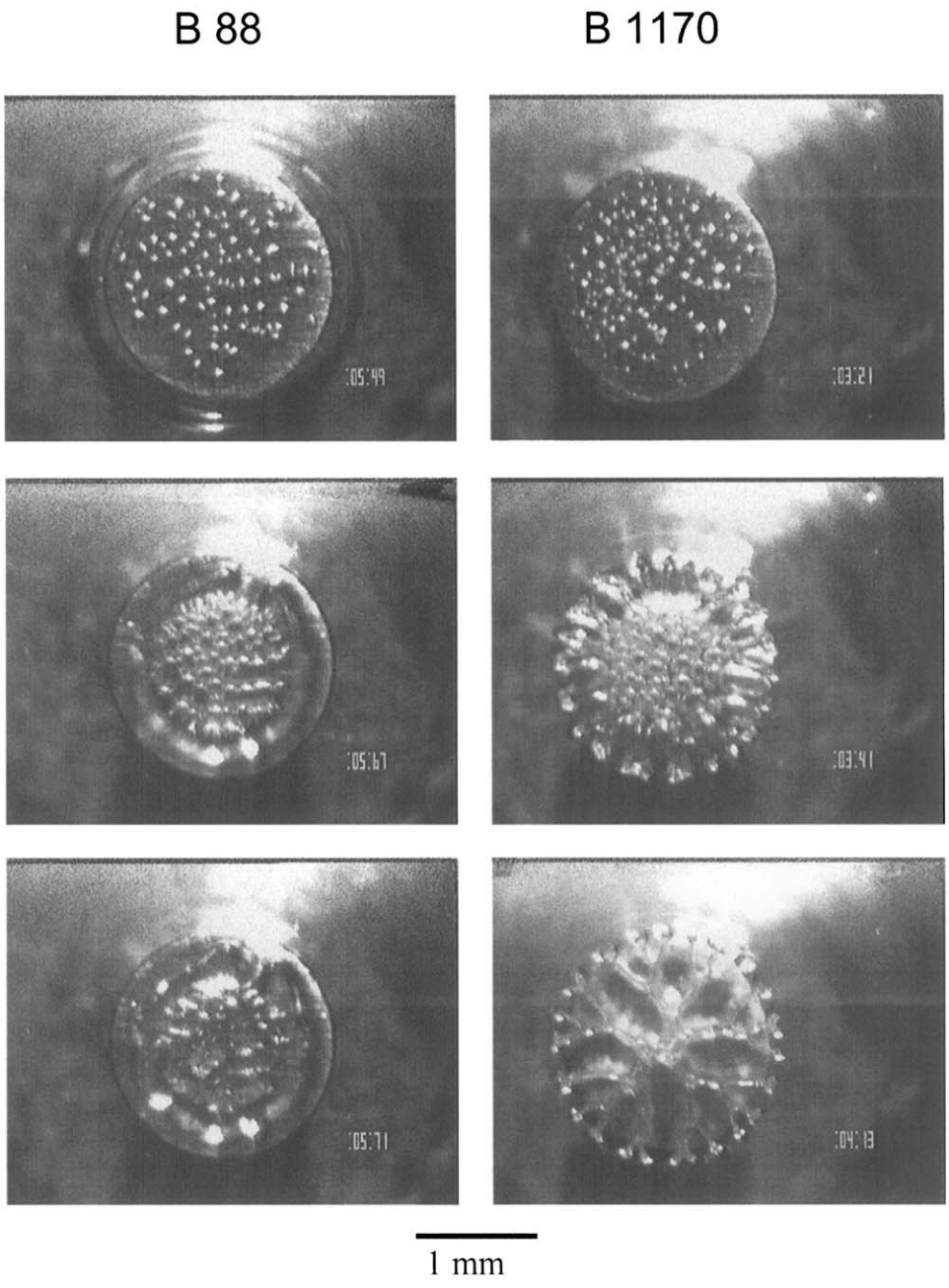

Fig. 8. Bottom view of the debonding pattern for 80/20 blends (a) B1/B88; (b) B1/B1170. Progression of images from top to bottom: 20 ms after first appearance of cavities, during growth of cavities, after debonding. Test conditions: $T=25°C$, $F_c=2\,N$, dwell-time $t_d=1\,s$, debonding rate $v_d=1\,mm/s$.

than at 25°C but the variation with molecular weight is less pronounced. On the other hand, ε_B at −10°C is always below that at 25°C except for the B88 sample which does not form fibrils at 25°C. Finally, for the low-molecular-weight blends (including B88 and B395), W_{adh} increases as temperature decreases due to the occurrence of fibrillation. For high molecular weights, where W_{adh} is dominated by fibrillation even at 25°C, little effect of temperature is seen. The increase in σ_s almost compensated by the loss in ε_B and the energy of adhesion at −10°C is only slightly higher than at 25°C.

4. Discussion

4.1. Initial contact and cavitation behavior

Adhesive tack is a function of two factors: the ability of the adhesive to spread and wet the probe, and the resistance of the adhesive to withdrawal. These are competing factors, since improving one generally has a negative effect on the other. Heterogeneities, for example air cavities, impair the strength of the adhesive bond by limiting contact. During contact between the

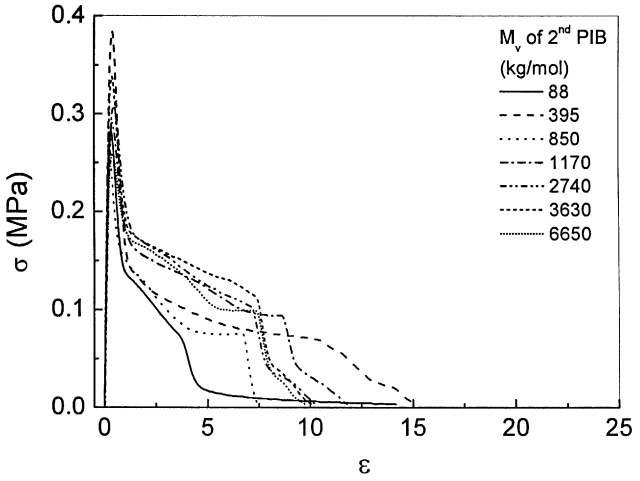

Fig. 9. Representative stress strain curves for Bl/BX blends with mixing ratio 80/20. Test conditions: $T=-10^{\circ}C$, $F_c=2\,N$, dwell-time $t_d=1\,s$, debonding rate $v_d=1\,mm/s$.

probe and adhesive, it can be assumed that there is some air trapped at the interface inside surface roughnesses [12].

Regardless of whether air is trapped at the interface, Gent and Tompkins [19] predicted that for a crosslinked rubber, voids must appear and grow inside the structure when it is subjected to a hydrostatic stress that exceeds its shear modulus. For a high-molecular-weight polymer, growth of these cavities is hindered by adhesive viscosity. Therefore, many small cavities will appear, decreasing the load-bearing area. In a low-viscosity adhesive, growth of these voids occurs more easily and there are expected to be fewer, larger cavities [20]. This prediction is consistent with the observed cavitation illustrated in Fig. 8: the first cavities formed in the 80/20 B1/B88 sample are larger in size than the numerous small cavities in the 80/20 B1/B1170 sample. The air bubbles expand as the adhesive around them is deformed. As the cavities increase in volume, their internal pressure may become lower than the outside pressure, causing them to act like microscopic "suction cups" [20,21], contributing to a greater work of adhesion.

Changing the contact force can significantly alter the response of the adhesive during withdrawal of the probe by changing the degree of contact and the amount of trapped air between the probe and adhesive. At low contact forces there is little effect of M_v on the initial stress peak σ_p. Higher contact force enhances the ability of the adhesive to spread, decreases the amount of air remaining between the probe and PSA, and thus increases the percentage of the probe area which is in intimate contact with adhesive. Accordingly, the number of cavities formed during debonding decreases as F_c increases (see left column Fig. 5). Increasing the contact force consistently increases the initial peak stress value σ_p for all molecular weights. But this effect is much more

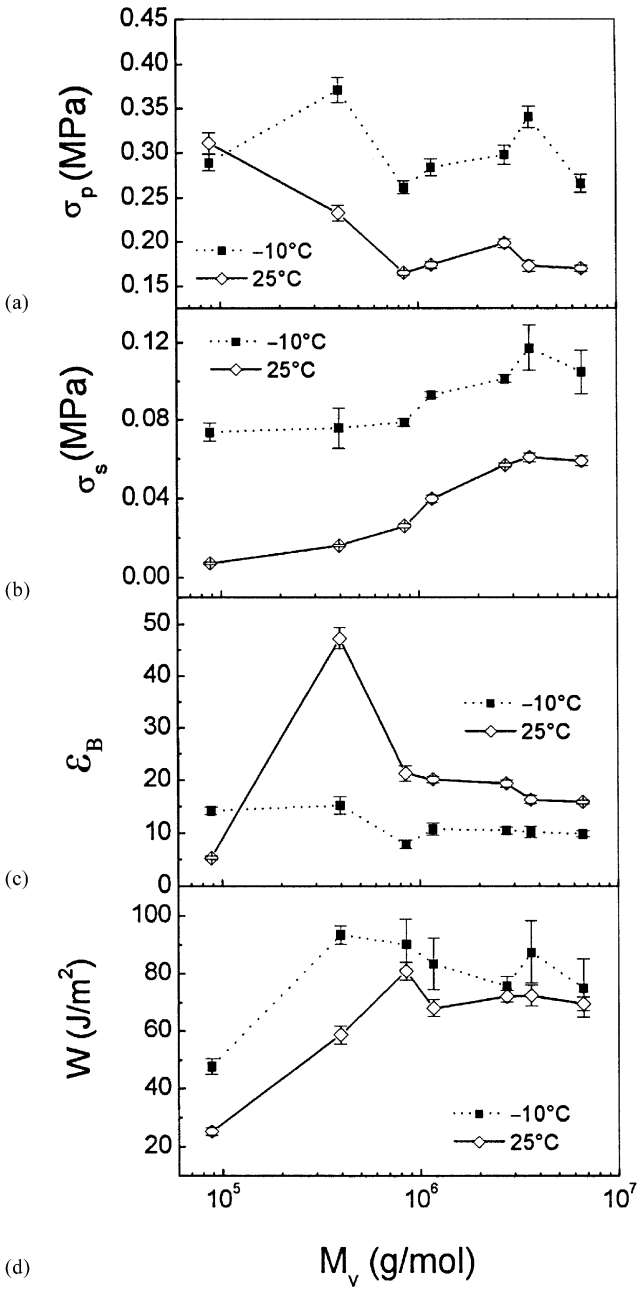

Fig. 10. Characteristic parameters σ_p, σ_s, ε_B, and W_{adh} of stress strain curve for the 80/20 blends Bl/BX as a function of M_v at $T=25^{\circ}C$ and $-10^{\circ}C$. Test conditions: $F_c=2\,N$, dwell-time $t_d=1\,s$, debonding rate $v_d=1\,mm/s$.

pronounced for the samples with low molecular weight (B88 and B395) and hence lower viscosity (see Fig. 7). In these cases the applied pressure can drive the polymer to flow into the bumps and voids of the probe thus increasing the contact area. At molecular weights beyond 3000 kg/mol the viscosity of the polymer is such high that a variation of the contact force from 0.5 to 5 N does not increase the contact area substantially. Note, the viscosity scales as $M^{3.4}$ and thus viscosity changes by

more than 6 orders of magnitude for the molecular weight range investigated here.

Contact formation directly determines the cavitation process, but as the number of cavities decreases in the early stage of debonding the number of fibrils formed in the later stage of debonding also decreases and the fibrillation pattern coarsens. This clearly shows up in the images presented in the right column of Fig. 5, which were taken just before failure. But this coarsening of the fibrillation pattern has not much impact on the stress during withdrawal and the parameters σ_s and ε_B do not change very much with applied contact force.

4.2. Fibrillation and molecular weight

The occurrence of a second peak or shoulder in the stress–strain diagram σ_s is characteristic of fibrillation, which allows for significant dissipation of energy. Fibrillation increases the work of adhesion above that due to the contributions of good initial wetting and initial resistance to flow. The extent of fibrillation also depends on the strength of the interfacial adhesive bond [22]. For a PSA with higher cohesive strength, the resistance to fibril elongation will rise more quickly, but its maximum value may depend on the interfacial bond with the probe. The height of σ_p for the low-molecular-weight samples B88 and B395 (Figs. 6(a) and 7) shows that they have strong surface adhesion, but they flow easily and therefore fail quickly during debonding, leading to a very low value of σ_s. For the B88 sample there is no visual evidence of any fibrillation. As soon as the air penetrates from the edges of the probe (at the small shoulder in σ as shown in Fig. 3), failure follows quickly. The film of B395 shows some fibrillation, but there are few thin strands, which extend to long distances (note the large error bars on the value of ε_B for this sample), indicating low cohesive strength and very poor properties. An adhesive with this behavior would aggressively stick to a surface but provide no strength for any application, and it would leave significant residue after removal. The high value of W_{adh} for these samples at 5.0 N contact force is a result of the large σ_p due to the intimate contact between these polymers and the probe. At lower contact forces, W_{adh} decreases drastically and becomes a more useful reflection of adhesive performance since the initial peak no longer dominates the area under the stress-strain curve.

A minimum molecular weight is required to get fibrillation. Only blends with molecular weight of 850 kg/mol or higher show true fibrillation. In this range, ε_B slightly decreases with increasing molecular weight, while σ_s strongly increases for M_v around 1000 kg/mol and tends to level off beyond 3000 kg/mol. In addition, a coarsening of the fibrillation pattern was observed with decreasing M_v, typical examples are shown in Fig. 11. A similar coarsening has been

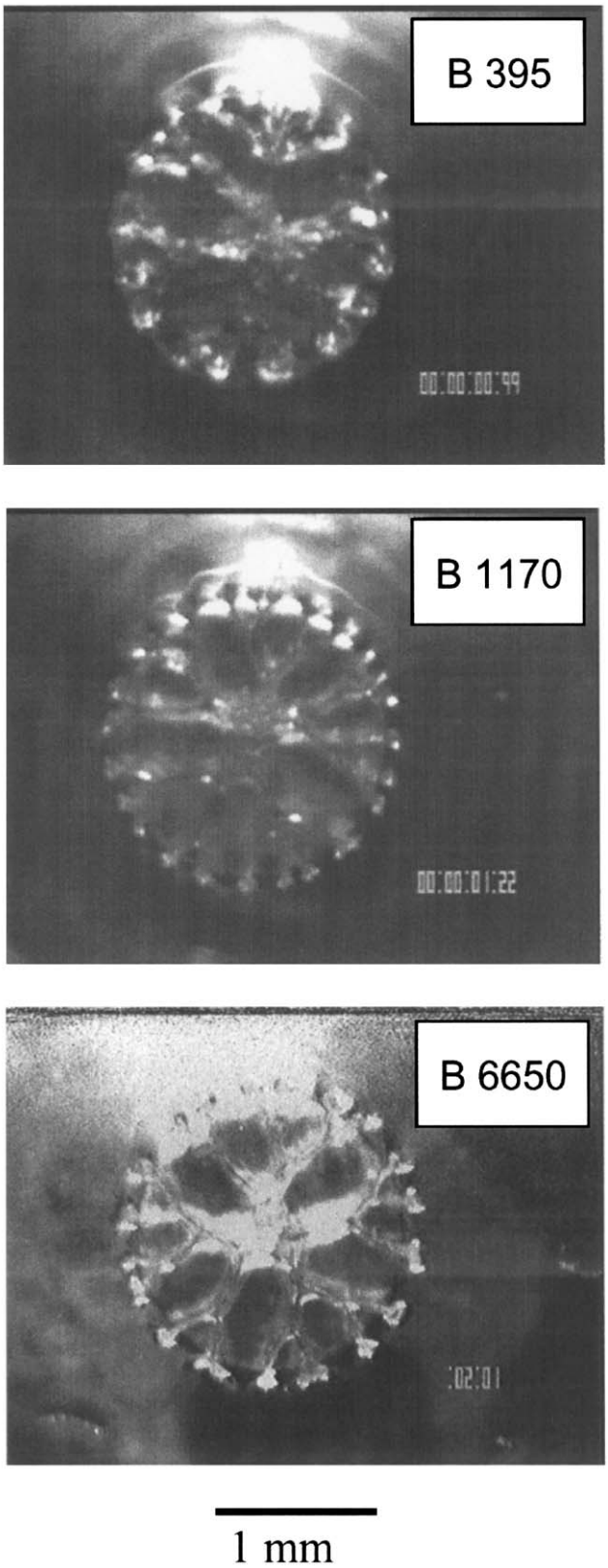

Fig. 11. Bottom view of the debonding pattern for 80/20 blends immediately after failure (top) B1/B395; (middle) Bl/1170; (bottom) B1/B6650. Test conditions: $T = 25°C$, $F_c = 2$ N, dwell-time $t_d = 1$ s, debonding rate $v_d = 1$ mm/s.

Table 2
Comparison of the stress required for fibril deformation σ_s and shear holding power for 80/20 blends of B1/BX as a function of M_v, (σ_s data from Fig. 10, $T = 25°C$)

M_v of 2nd PIB (kg/mol)	σ_s (kPa)	Holding time (s)	Shear failure mode
88	7.4	0	Cohesive
395	16.3	10	Cohesive
850	26.4	10	Cohesive
1170	40.1	60	Cohesive
2740	56.9	90	Cohesive
3630	60.8	120	Adhesive/ cohesive
6650	58.9	120	Adhesive/ cohesive

observed with increasing contact force (Fig. 5). Nevertheless, σ_s and ε_B both turned out to be essentially independent of contact force. Therefore, we conclude that the fibrillation pattern (many thin fibrils or few fibrils with large cross-section) is not the reason for the change in σ_s and ε_B. Instead, these parameters characterize the intrinsic cohesive strength of the polymer, and qualitatively, the observed dependence on molecular weight reflects the increased resistance of the polymer to deformation due to the increasing viscosity and the increasing number of entanglements per molecule as M_v increases.

The information on cohesive strength gained from tack tests also corresponds to measurements of shear holding power. The holding time depends on the internal structural resistance of the PSA to a shear stress. A greater number of entanglements inhibits elongation and improves an adhesive's shear strength or holding power. During a tack test, the stress σs, which is necessary to elongate the fibrils, is also an indication of cohesive strength. A high stress level thus corresponds to a longer holding time. This is confirmed by the comparison of the molecular weight dependency of σs and the shear strength (as measured in a standard shear holding power test) of the 80/20 model blends as depicted in Table 2. These samples failed very quickly, due to the fact that they are not true formulated adhesives. The first several samples failed cohesively. The final two samples showed areas of cohesive failure as well as areas of adhesive failure. Increasing cohesive strength thus made failure less likely to occur within the film itself; this is also predicted from the smaller ε_B and larger σ_s values. Shear strength is directly related to the zero-shear viscosity and the number of entanglements [10], so the increased number of entanglements at higher molecular weight logically corresponds to the increased shear holding power observed.

4.3. Effect of temperature

The glass-transition temperature of a PSA should be high enough to provide resistance to flow in short-time tests, but low enough to prevent a glassy or brittle response. Zosel has shown that tack properties for acrylic PSAs are best at temperatures around 50–70°C above the glass-transition temperature [5]. If this holds true for PIB, which has a T_g of −65°C (see Fig. 1), optimum properties would be expected in the range of −15–5°C. Cohesive strength increases as the material is brought closer to its T_g, reflected in the shear storage modulus, G', which increases sharply as T_g is approached.

Peak stress is a function of the wetting characteristics (improved at higher temperature and lower molecular weight) and of the resistance to flow (improved at lower temperature and higher molecular weight). Our data presented in Fig. 10 show that the initial stress peak σ_p is higher at −10°C as compared to 25°C irrespective of molecular weight, except for the very first data point. The effect of temperature is much more pronounced than the weak variations with M_v. This supports the observation of Creton [18] that for PSAs of high molecular weight, σ_p is strongly influenced by G'. The storage moduli for all samples are higher at −10°C than 25°C; but at room temperature and below, the storage moduli are independent of molecular weight.

Deformation of fibrils is also strongly dependent on temperature and modulus. As temperature is lowered, the stress σ_s to deform the fibrils increases, but at the same time failure occurs earlier. Finally, the effect of these two parameters on the total work of adhesion cancels and W_{adh} is only slightly higher at −10°C than at 25°C, mainly due to the (small) contribution of the initial stress peak of σ_p.

5. Conclusions

Polyisobutylene blends provide a good model system to study the effect of molecular weight on adhesive tack properties of non-crosslinked polymer materials. Pure PIB shows brittle fracture for $M_v > M_e$ but the addition of a low molecular weight component can be used to increase M_e and to drop G' below the Dahlquist criterion. Blends with a mixing ratio of 80/20 low to high molecular weight exhibit distinct cavitation and fibrillation and are well suited to study the effect of molecular weight on these properties in a wide range. These model systems are soft adhesives, achieving significant initial tack within a short contact period. Due to the absence of chemical crosslinking they show poor cohesive strength, as exemplified by the high final elongation values. Nevertheless, several conclusions are drawn from the investigation of these model systems, which should also hold for other PSA materials with more complicated molecular architecture.

Changing the tack test parameters caused different characteristics to be emphasised. The initial peak force is

a function of both cohesive strength and ability to wet the test probe. Increasing the contact force increases the importance of wetting, leading to very high σ_p and exaggerated W_{adh} especially for the low-molecular-weight samples. The deformation of the fibrils and hence the parameters σ_s and ε_B are much less sensitive to the initial contact force. To avoid overweighing of the wetting contribution and to get tack data reflecting the true application properties of PSA materials, we have thus focused on low or moderate contact force measurements to investigate the effect of molecular weight and temperature on adhesion.

Increasing molecular weight increases cohesive strength and leads to fibrillation. A minimum molecular weight of about 850 kg/mol is required to obtain stable fibrils. Further increasing M_v leads to a strong increase in σ_s until it tends to level off around 3000 kg/mol, while ε_B slightly decreases in this molecular weight range. These trends are found at 25°C as well as −10°C, but at lower temperature the values for σ_s are higher and those for ε_B are lower as compared to 25°C. All these findings directly correlate to the rheological properties of the polymer. Its viscosity increases with increasing molecular weight and decreasing temperature and the number of entanglements per polymer chain goes up with increasing molecular weight. Moreover, the parameters σ_s and ε_B are independent of the fibrillation pattern, the deformation of many thin fibrils seems to consume as much energy as the deformation of few thick fibrils. Finally, the work of adhesion is essentially independent of molecular weight and temperature in the "fibrillation-controlled" regime above $M_v \approx 850$ kg/mol.

Acknowledgements

We would like to thank C.W. Macosko (University of Minnesota) for many fruitful discussions and for his support throughout the PhD project of AEO. The assistance of H. Schoch and D. Lingenfelder in performing the experiments is gratefully acknowledged.

References

[1] Dahlquist CA. In: Patrick RL, editor. Treatise on adhesion and adhesives. New York: Marcel Dekker; 1969. p. 244–9.
[2] Benedek I, Heymans LJ. Pressure-sensitive adhesives technology. New York: Marcel Dekker; 1997.
[3] Creton C. In: Meijer HJ, editor. Materials science and technology, vol. 18. Weinheim, Germany: VCH; 1997. p. 708–41.
[4] Hammond FHJ. In: Satas D, editor. The handbook of pressure-sensitive adhesive technology. 2nd ed. New York: Van Nostrand Reinhold; 1989. p. 38–60.
[5] Zosel A. Colloid Polym Sci 1985;263:541–53.
[6] Tse MF, Jacob L. J Adhes 1996;56:79–95.
[7] Gent AN, Schultz J. J Adhes 1972;3:281.
[8] Zosel A. J Adhes 1989;30:135–49.
[9] Satas D. In: Satas D, editor. Handbook of pressure-sensitive adhesive technology. 2nd ed. New York: Van Nostrand Reinhold; 1989. p. 1–23.
[10] Tobing SD, Klein A. J Appl Polym Sci 2001;79:2230–44.
[11] Tobing SD, Klein A. J Appl Polym Sci 2001;79:2558–64.
[12] Zosel A. Int J Adhes Adhes 1998;18:265–71.
[13] Higgins JJ, Jagisch FC, Stucker NE. In: Skeist I, editor. Handbook of adhesives, 3rd ed. New York: Van Nostrand Reinhold; 1990; 239–58.
[14] Crosby AJ, Shull KR. J Polym Sci Part B: Polym Phys 1999;37:3455–72.
[15] Zosel A. Adhesives & Sealant Industry 2000;7(9):30–6.
[16] Dahlquist CA. In: Adhesion fundamentals and practice. London: McLaren and Sons Ltd.; 1996. p. 143–51.
[17] Lakrout H, Creton C, Ahn D, Shull KR. Macromolecules 2001;34:7448–58.
[18] Lakrout H, Sergot P, Creton C. J Adhes 1999;69:307–59.
[19] Gent AN, Tompkins DA. J Polym Sci Part A-2: Polym Phys 1969;7:1483.
[20] Gay C, Leibler L. Phys Today 1999;52(11):48–52.
[21] Gay C, Leibler L. Phys Rev Lett 1999;82:936–40.
[22] Good RJ, Gupta RK. J Adhes 1988;26:13–36.